

**A Reduction Series of Neodymium Supported by
Pyridine(diimine) Ligands**

Journal:	<i>Dalton Transactions</i>
Manuscript ID	DT-COM-02-2019-000679.R2
Article Type:	Communication
Date Submitted by the Author:	05-Apr-2019
Complete List of Authors:	Galley, Shane; Purdue University, Chemistry Pattenaude, Scott; Purdue University, Chemistry Higgins, Robert; University of Pennsylvania, Department of Chemistry Tatebe, Caleb; Purdue University, Chemistry Stanley, Dalton; Purdue University, Chemistry Fanwick, P; 1393 Brown Building, Department of Chemistry Zeller, Matthias; Purdue University, Department of Chemistry Schelter, Eric J; University of Pennsylvania, Department of Chemistry Bart, Suzanne; Purdue University, Chemistry;

COMMUNICATION

A Reduction Series of Neodymium Supported by Pyridine(diimine) Ligands

Received 00th January 20xx,
Accepted 00th January 20xx

Shane S. Galley,^a Scott A. Pattenaupe,^a Robert F. Higgins,^b Caleb J. Tatebe,^a Dalton A. Stanley,^a Phillip E. Fanwick,^a Matthias Zeller,^a Eric J. Schelker,^b and Suzanne C. Bart*^a

DOI: 10.1039/x0xx00000x

Dedicated to Professor Geoff Cloke on the occasion of his 65th birthday

The synthesis of a redox series of neodymium species bearing the redox active pyridine(diimine) ligand, ^{Mes}PDI^{Me}, is reported. Spectroscopic and structural characterization supports each compound has a Nd(III) centre, with the ^{Mes}PDI^{Me} ligand existing in four oxidation states.

Redox active ligands have been used to generate unique metal species from every area of the periodic table. These ligands are known for their ability to stabilize electron rich metal centres,¹ facilitate multi-electron chemistry,^{2, 3} and create compounds with interesting electronic structures.^{4, 5} Such properties are particularly attractive to confer to the lanthanide elements, as these metals typically prefer the +3 oxidation state. Fedushkin has been quite active in this field, using a variety of redox-active ligands on metals throughout the lanthanide series. In one recent example, this research group reported the synthesis of a series of lanthanide derivatives of the 1,2-bis[[2,6-diisopropylphenyl]imino]-acenaphthene (dpp-Bian) ligand in three different redox states.⁶⁻⁹ Gambarotta has also shown the versatility of the pyridine(diimine) ligand, ^{DIPP}PDI^{Me} (2,6-[2,6-diisopropylphenyl]-N=C(Me)₂C₅H₃N), to support neodymium centres.^{10, 11} Metallation with Nd⁰ in the presence of I₂ forms (^{DIPP}PDI^{Me})NdI₂, which was characterized as a neodymium(III) centre with a ligand radical, [^{DIPP}PDI^{Me}][•]. Mazzanti and co-workers have shown that Schiff base ligands can store electrons in a carbon-carbon bond, supporting a variety of lanthanides, including Nd, Tb, Eu, Yb.¹²

Recent work from our group demonstrated that using the bis(iminoquinone) ligand scaffold and its reduced forms on neodymium centres facilitated multielectron redox reactivity. In this case, two reduced ligands of [K(18-c-6)][(^{DIPP}ap)₂Nd(THF)₂] (^{DIPP}ap = 4,6-di-*tert*-butyl-2-(2,6-diisopropylphenyl)-amidophenolate) were simultaneously oxidized by either

sulphur and selenium, forming unusual twist boat metalacyclic structures supported by iminosemiquinone ligands, [(^{DIPP}isq)₂NdS₅] and [(^{DIPP}isq)₂NdSe₅].¹³ We hypothesized that using a ligand capable of storing additional reducing equivalents may create more potent reductants for future multi-electron redox-chemistry. Herein, a series of reduced neodymium complexes featuring the redox-active pyridine(diimine) ligand, ^{Mes}PDI^{Me}, is reported. Spectroscopic and structural characterization were used to fully assign the ligand and neodymium oxidation states.

The first entry in the neodymium series was targeted by treating a toluene solution of NdI₃(THF)_{3,5} with a single equivalent of ^{Mes}PDI^{Me} ligand. After stirring and workup, a yellow powder was isolated (Scheme 1). Analysis of a CD₃CN solution of this material by ¹H NMR spectroscopy displayed a paramagnetically broadened and shifted spectrum with nine resonances ranging from -4 to 15 ppm, which is expected due to the f³ Nd(III) ion. Analysis of single crystals of this compound obtained from CH₂Cl₂ aided in the assignment as (^{Mes}PDI^{Me})Nd(I)₃(THF) (**Nd-I₃**) (Figure S3), with one ^{Mes}PDI^{Me} ligand, one THF co-ligand, and three iodine atoms in meridional fashion around a seven-coordinate, pentagonal bipyramidal Nd centre. The Nd-I bond lengths (3.0514(6), 3.0861(6), 3.0890(6) Å) are consistent with other Nd(III) complexes,^{13, 14} while the Nd-O_{THF} distance (2.450(3) Å) is similar to Nd-O_{THF} bond lengths previously reported.¹⁴ Examination of the intraligand bond

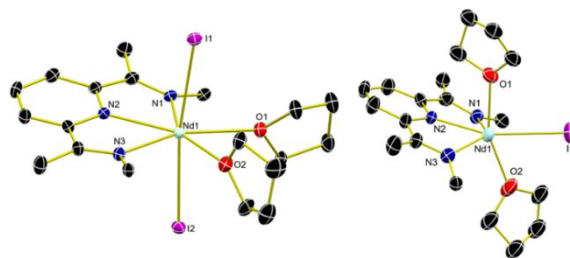
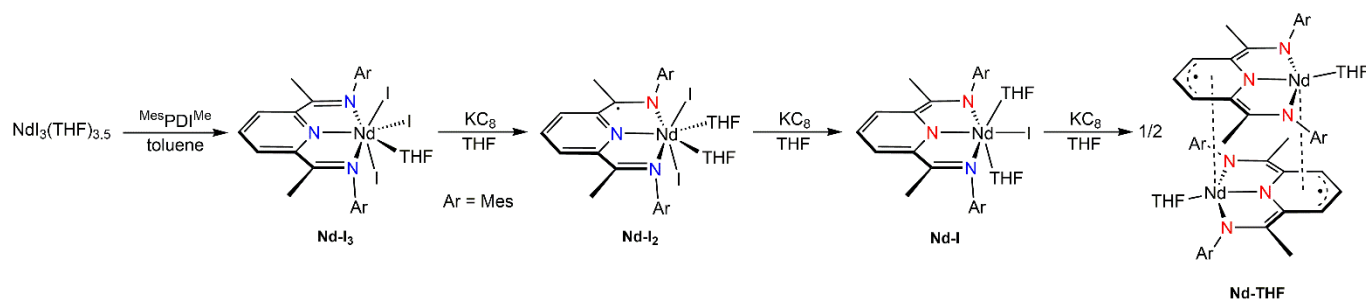


Figure 1. Molecular structures of **Nd-I₂** (left) and **Nd-I** (right) shown as 30% probability ellipsoids. Co-crystallized solvent molecules, mesityl groups, and hydrogen atoms have been omitted for clarity. An image without truncation can be found in the SI.

^a H. C. Brown Laboratory, Department of Chemistry, Purdue University, West Lafayette, IN 47906, United States.

^b P. Roy and Diana T. Vagelos Laboratories, Department of Chemistry, University of Pennsylvania, 231 S. 4th Street, Philadelphia, PA 19104, United States.

†Electronic Supplementary Information (ESI) available: ¹H NMR spectroscopic data, experimental details, crystallographic data, electronic absorption spectra. See DOI: 10.1039/x0xx00000x

Scheme 1. Synthesis of **Nd-I₃**, **Nd-I₂**, **Nd-I**, **Nd-THF**

lengths, when compared to the free ligand shows no reduction has occurred,¹⁵ as the C-N_{imine} bond lengths in **Nd-I₃** (1.279(6), 1.272(6) Å) are the same as those for ^{Mes}PDI^{Me} (1.277(3), 1.276(3) Å).

To engage the redox activity of the ligand, the first reduced compound was synthesized by addition of one equiv of KC₈ to a THF solution of **Nd-I₃**. An immediate colour change from yellow to orange was observed. After one hour of stirring, the reaction mixture was worked-up to remove graphite and KI. Drying resulted in an orange powder (Scheme 1). The ¹H NMR spectrum (C₆D₆) of this material displayed broad resonances in the range -238 to 190 ppm (Figure S4); a large spectroscopic window such as this can signify the presence of a ligand radical. This has previously been noted for (^{Mes}PDI^{Me})U₃, which contains a tetravalent uranium centre and a [^{Mes}PDI^{Me}]⁻¹ ligand.²

To confirm ligand reduction, single crystals suitable for X-ray diffraction were grown from a concentrated C₆H₆ solution at room temperature. Refinement of these data revealed a seven-coordinate, pentagonal bipyramidal Nd centre (Figure 1, left). The molecular structure shows two iodine atoms, two THF molecules, and one tridentate ^{Mes}PDI^{Me} ligand consistent with ^{Mes}PDI^{Me}NdI₂(THF)₂ (**Nd-I₂**). The neodymium-iodide bond lengths (Nd-I = 3.1203(6), 3.1243(6) Å) are similar to those reported for Tp*NdI₂(THF) (Tp* = hydrotris(3,5-dimethylpyrazolyl)borate; Nd-I = 3.040(2), 3.055(2) Å).¹⁴ The neutral Nd-O_{THF} bond lengths (2.568(5), 2.533(5) Å) are consistent with other Nd-O_{THF} distances ([1,4-diaza-1,3-butadiene]NdI(THF)₃ = 2.470(6)-2.582(5) Å).¹⁶ The Nd-N_{imine} bond lengths (2.576(5), 2.598(5) Å) are similar to ^{DIPP}PDI^{Me}NdI₂(THF) (Nd-N = 2.479(7), 2.555(7) Å) reported by Gambarotta and co-workers.¹⁰ These Nd-N_{imine} bond lengths are markedly longer than **Nd-I₂**'s Nd-N_{pyr}, which is 2.417(5) Å. Both C-N_{pyr} bonds are statistically identical (1.383(8), 1.395(8) Å) (Figure 3), and are also consistent with those reported for ^{DIPP}PDI^{Me}NdI₂(THF) (N-C = 1.307(11), 1.352(11) Å).¹⁰

Further reduction of **Nd-I₂** was possible by treating one equiv of this material with an equiv of KC₈, which produced a dark yellow solution. Work-up of this reaction followed by drying afforded a red-brown powder, which was then crystallized from a cold, concentrated diethyl ether solution (Scheme 1). Examination of a C₆D₆ solution of this powder by ¹H NMR spectroscopy revealed full conversion of **Nd-I₂**, but the broad, paramagnetic features of the spectrum (range: -9 to 191 ppm) did not allow for a structural assignment via this method (Figure S5). Fortunately, X-ray crystallography analysis of the

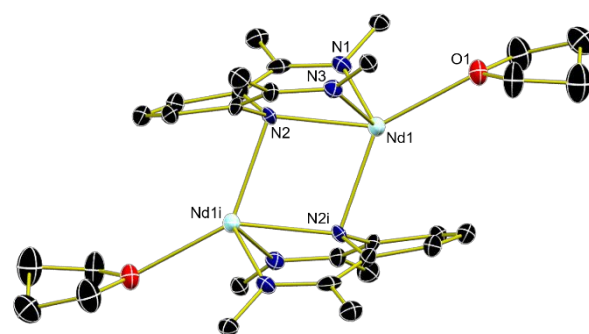


Figure 2. Molecular structure of **Nd-THF** shown as 30% probability ellipsoids. Co-crystallized solvent molecules, mesityl groups, and hydrogen atoms have been omitted for clarity. An image without truncation can be found in the SI.

dark orange crystals was possible, and a six-coordinate pseudo-octahedral Nd complex was revealed and assigned as ^{Mes}PDI^{Me}NdI(THF)₂ (**Nd-I**) (Figure 1, right). The Nd-I bond length (3.257(3) Å) is similar to (^{DIPP}isq)₂NdI(THF) (^{DIPP}isq = 4,6-di-*tert*-butyl-2-(2,6-diisopropylphenyl)iminosemiquinone; Nd-I = 3.0724(11) Å).¹³ Both the Nd-N_{pyr} (2.332(9) Å) and Nd-N_{imine} (2.384(9), 2.459(10) Å) bond lengths have contracted with respect to those observed in **Nd-I₂**. The shorter bond lengths are similar to the Nd-N bond lengths reported for [K(18-c-6)][(^{DIPP}ap)₂Nd(THF)₂] (Nd-N = 2.4378(19) Å),¹³ while the other Nd-N bond length is closer to the Nd-N_{amide} bond length for di[bis-4,4'-(1,3-propanediylidimino)-3-pentene-2-onato]-Nd(N(SiMe₃)₂) (2.350(2) Å).¹⁷ A characteristic bond elongation seen in both C-N_{pyr} bonds (1.417(14), 1.418(14) Å) are roughly 0.02 Å longer than the same bonds seen for **Nd-I₂** (Figure 3).

To study the extent of reduction possible with this ligand framework, **Nd-I** was treated with an equiv of KC₈. During the reaction, the colour of the mixture progressed from brown-green to green (Scheme 1). A pure solid was obtained after workup, and the ¹H NMR spectrum of this material showed chemical shifts in the range of -479 to 227 ppm. To discern the structural assignment of this isolated green powder, crystals obtained from this material were analysed by X-ray crystallography. Analysis showed a dimeric complex, specifically [^{Mes}PDI^{Me}Nd(THF)]₂ (**Nd-THF**). The Nd-N_{imine} bond lengths (2.447(6), 2.459(5) Å) are shorter than the Nd-N_{imine} bond lengths for **Nd-I**. An examination of the pyridine ring displays a Nd-N_{pyr} bond length (2.346(5) Å) which is similar to **Nd-I** and ^{DIPP}PDI^{Me}NdI₂(THF) (2.376(7) Å).¹⁰ Interestingly, the pyridine nitrogen is bonded to the opposite neodymium centre, and is pulled out of the plane of the remaining carbon atoms sitting 0.468 Å below the plane. This pyridine interaction reinforces the

dimeric structure observed here.

Comparison of the intraligand distances is also a useful indicator that supports ligand reduction. This methodology has been previously established for main group and transition metals,¹⁸ lanthanides, and actinides. For the pyridine(diimine) ligand family specifically, ligand reduction generally causes structural distortions in the imine arms, the adjacent carbon-

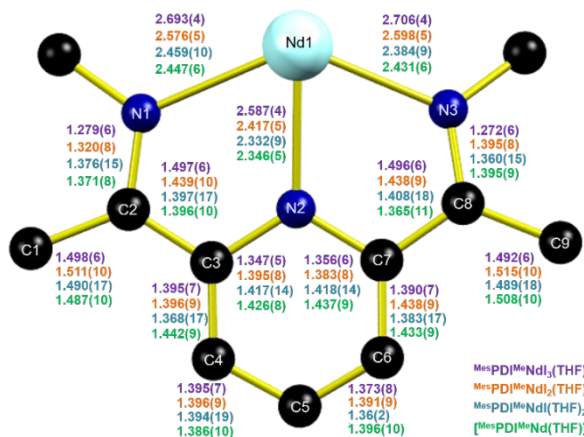


Figure 3. Selected bond lengths of **Nd-I₃** (purple), **Nd-I₂** (orange), **Nd-I** (blue), and **Nd-THF** (green), in Å.

carbon bond, and in some cases, the pyridine ring, as compared to **Nd-I₃**. Figure 3 presents selected intraligand bond distances for the new neodymium family, **Nd-I₂**, **Nd-I**, and **Nd-THF**. Starting with **Nd-I₂**, it is possible to see elongation in the C-N_{imine} bond distances as compared to the distances of **Nd-I₃** (1.272(6), 1.279(6) Å). In this case, the imine arms are elongated in an inequivalent fashion, indicating localization of the ligand radical, and formulation as a Nd(III) centre with a [MesPDI^{Me}]¹⁻ ligand radical. This is supported by the adjacent C-C bond, which has now been contracted to 1.439(10) and 1.438(9) Å from 1.497(6) Å in **Nd-I₃**. Even more distortion is noted for **Nd-I**, which is consistent with additional ligand reduction. In this case, the C-N_{imine} distances are elongated further and the adjacent C-C bond is contracted more severely, consistent with an Nd(III)-[MesPDI^{Me}]²⁻ formulation. Finally, **Nd-THF**, shows the most extensive reduction, with the C-N_{imine} bond distances elongated to 1.371(8) and 1.395(9) Å and the C-C distance contracted to 1.396(10) and 1.365(11) Å. In the latter case, the dimer can be assigned as a Nd(III) center with a trianionic MesPDI^{Me} ligand. Although previously thought to be rare, observations of the trianionic form are becoming more prevalent, with examples for both transition metals¹⁹ and uranium,^{2, 4, 20} and now also the lanthanide, Nd.

Magnetic susceptibility data were collected to support the assignment of the redox states of the Nd cations and MesPDI^{Me} ligands for **Nd-I₃**, **Nd-I₂**, **Nd-I** and **Nd-THF** (Figure 4 and Table 1). Complex **Nd-I₃** displayed a room temperature moment of $\mu_{\text{eff}} = 3.95$ which slowly decreased with temperature until 2 K where a value of $\mu_{\text{eff}} = 2.55$ was attained. These susceptibility data were indicative of a Nd³⁺ oxidation state (⁴I_{9/2} ground state, Curie value $\mu_{\text{eff}} = 3.62$) and a neutral MesPDI^{Me} ligand, which was consistent with other Nd³⁺, closed shell ligand complexes (*i.e.*, Nd(DOPO)₃, DOPO = 2,4,6,7-tetra-*tert*-butyl-1-oxo-1*H*-phenox-

azin-9-olate, $\mu_{\text{eff}} = 3.62$ and 1.97 at 300 and 2 K, respectively).^{21, 22} The susceptibility and magnetization data for **Nd-I** were similar to **Nd-I₃** (Table 1), and were also consistent with a Nd³⁺ ion and a closed-shell, dianionic PDI²⁻ ligand.

The bis-iodide complex **Nd-I₂** displayed larger susceptibility values across all temperatures compared to **Nd-I₃** and **Nd-I**, consistent with a [MesPDI^{Me}]¹⁻ ligand with a ligand radical. This was further supported by saturation of magnetization experiments at 2 K that showed a difference in the magnetization

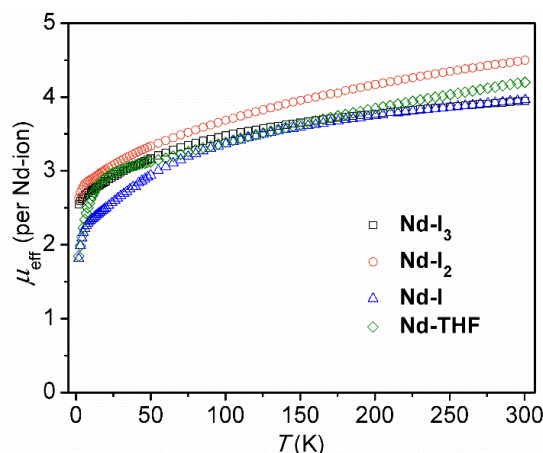


Figure 4. Temperature dependence of the magnetic moment for **Nd-I₃**, **Nd-I₂**, **Nd-I** and **Nd-THF**.

value at 70 kOe of $\sim 1 \mu_{\text{B}}$ compared to **Nd-I₃** and **Nd-I**, which lacked ligand radicals. The magnetic properties of **Nd-I₂** were similar to those previously reported by Gambarotta, Möller and Budzelaar for the related ^{DIPP}PDI^{Me}Nd(I)₂(THF), where $\mu_{\text{eff}} = 4.63$ and 2.87 at 300 and 2 K, respectively.²³ Temperature dependent μ_{eff} data for **Nd-THF** displayed values consistent with two Nd³⁺ ions and two ligand radicals. The downturn at low temperatures (Fig. 4) is presumably due to weak antiferromagnetic interactions between Nd ions and ligand radicals. The observation of a paramagnetic response from [MesPDI^{Me}]³⁻ is different than what was observed for the dimeric U(IV) complex, [MesPDI^{Me}U(II)]₂,²⁴ but in agreement with other trianionic [MesPDI^{Me}]³⁻ ligands bound to alkali and transition metals.^{25, 26} In total, these data are consistent with the redox states assigned for each complex according to the structural parameters obtained from X-ray crystallography.

The neodymium compounds reported here were also analysed using solution phase electronic absorption spectroscopy in the UV-visible regions. Data for **Nd-I₃**, **Nd-I₂**, **Nd-I**, and **Nd-THF** were collected from 300 to 800 nm at ambient temperature in THF (**Nd-I₂**, **Nd-I**, and **Nd-THF**) or acetonitrile (**Nd-I₃**) (Figures S2, S5, S7, S9). Spectroscopic and structural parameters indicate that **Nd-I₂** contains a ligand radical, [MesPDI^{Me}]¹⁻, thus its absorption spectrum is unique as compared

Table 1. Selected magnetic properties for **Nd-I₃**, **Nd-I₂**, **Nd-I**, and **Nd-THF**.

Complex	μ_{eff} at 300 K	μ_{eff} at 2 K	M (μ_{B}) at 2K, 70 kOe
Nd-I₃	3.95	2.55	1.37
Nd-I₂	4.50	2.63	2.10

Nd-I	3.96	1.81	0.90
Nd-THF	5.94 (4.20) ^a	2.61 (1.84) ^a	3.95 (1.98) ^a

^avalue is considered on a per-Nd ion basis

to the rest of the series. Inspection of the UV and visible regions for **Nd-I₃** indeed show a more pronounced absorption profile as compared to **Nd-I₂**, **Nd-I**, and **Nd-THF**. In this case, an intense absorption was noted at 359 nm, likely due to ligand $\pi\text{-}\pi^*$ transfers into the empty π^* orbital. In a striking contrast to **Nd-I₃**, the absorption spectra for **Nd-I₂**, **Nd-I**, and **Nd-THF** are relatively broad and rather featureless; the well-defined bands for **Nd-I₃** are absent in these cases due to the population of the π^* orbitals with electrons that makes electron transfers more difficult. Both **Nd-I₂** and **Nd-I** show molar absorptivities ranging on the scale of 0-8000 M⁻¹cm⁻¹, as well as colour-producing bands around 500 nm that are responsible for the dark orange colours of these compounds. Interestingly, **Nd-THF** shows absorptions as high as ~25,000 M⁻¹cm⁻¹, with a pronounced absorption at 363 nm, likely attributed to ligand $\pi\text{-}\pi^*$ absorptions. The resonance around 650 nm indicates absorption in the red and emission in the green, ultimately responsible for the emerald green colour of this solution. Overall, the absorption data is consistent with neodymium(III) compounds with reduced ligands, except in the case of **Nd-I₃**.

Conclusions

In summary, we report the synthesis of a series of electron-rich neodymium species supported by the redox-active pyridine(diimine) ligand, ^{Mes}PDI^{Me}. Sequential reductions were achieved using potassium graphite. Spectroscopic and structural characterization confirmed that reduction occurs at the ligand rather than the neodymium centre, maintaining the Nd +3 oxidation state. These species are intriguing as they are masked forms of low-valent neodymium centres which may ultimately result in reactive molecules. Future studies will be aimed at exploring the multi-electron redox chemistry of these derivatives.

Conflicts of interest

There are no conflicts to declare.

Acknowledgements

This work was funded by the Division of Chemical Sciences, Geosciences, and Biosciences, Office of Basic Energy Sciences Heavy Elements Chemistry program through grant DE-SC0008479 (SCB) and the Separations and Analysis program of the U.S. Department of Energy program through grant DE-SC0017259 (EJS) for financial support. R.F.H. and E.J.S. thank the NatureNet Science Fellowship program from The Nature Conservancy for support.

Notes and references

1. K. J. Blackmore, J. W. Ziller and A. F. Heyduk, *Inorg Chem*, 2005, **44**, 5559-5561.
2. N. H. Anderson, S. O. Odoh, Y. Yao, U. J. Williams, B. A. Schaefer, J. J. Kiernicki, A. J. Lewis, M. D. Goshert, P. E. Fanwick, E. J. Schelter, J. R. Walensky, L. Gagliardi and S. C. Bart, *Nat Chem*, 2014, **6**, 919-926.
3. J. J. Kiernicki, M. G. Ferrier, J. S. Lezama Pacheco, H. S. La Pierre, B. W. Stein, M. Zeller, S. A. Kozimor and S. C. Bart, *J Am Chem Soc*, 2016, **138**, 13941-13951.
4. N. H. Anderson, S. O. Odoh, U. J. Williams, A. J. Lewis, G. L. Wagner, J. Lezama Pacheco, S. A. Kozimor, L. Gagliardi, E. J. Schelter and S. C. Bart, *J Am Chem Soc*, 2015, **137**, 4690-4700.
5. P. J. Chirik, *Angew Chem Int Ed*, 2017, **56**, 5170-5181.
6. I. L. Fedushkin, A. N. Lukoyanov and E. V. Baranov, *Inorg Chem*, 2018, **57**, 4301-4309.
7. I. L. Fedushkin, O. V. Maslova, E. V. Baranov and A. S. Shavyrin, *Inorg Chem*, 2009, **48**, 2355-2357.
8. I. L. Fedushkin, O. V. Maslova, A. G. Morozov, S. Dechert, S. Demeshko and F. Meyer, *Angew Chem Int Ed*, 2012, **51**, 10584-10587.
9. I. L. Fedushkin, D. S. Yambulatov, A. A. Skatova, E. V. Baranov, S. Demeshko, A. S. Bogomyakov, V. I. Ovcharenko and E. M. Zueva, *Inorg Chem*, 2017, **56**, 9825-9833.
10. H. Sugiyama, I. Korobkov, S. Gambarotta, A. Möller and P. H. M. Budzelaar, *Inorg Chem*, 2004, **43**, 5771-5779.
11. H. Sugiyama, S. Gambarotta, G. P. A. Yap, D. R. Wilson and S. K. H. Thiele, *Organometallics*, 2004, **23**, 5054-5061.
12. C. Camp, V. Guidal, B. Biswas, J. Pécaut, L. Dubois and M. Mazzanti, *Chemical Science*, 2012, **3**, 2433-2448.
13. E. J. Coughlin, M. Zeller and S. C. Bart, *Angew Chem Int Ed*, 2017, **56**, 12142-12145.
14. D. P. Long, A. Chandrasekaran, R. O. Day, P. A. Bianconi and A. L. Rheingold, *Inorg Chem*, 2000, **39**, 4476-4487.
15. J. J. Kiernicki, B. S. Newell, E. M. Matson, N. H. Anderson, P. E. Fanwick, M. P. Shores and S. C. Bart, *Inorg Chem*, 2014, **53**, 3730-3741.
16. T. K. Panda, H. Kaneko, K. Pal, H. Tsurugi and K. Mashima, *Organometallics*, 2010, **29**, 2610-2615.
17. S. A. Schuetz, M. A. Erdmann, V. W. Day, J. L. Clark and J. A. Belot, *Inorg Chim Acta*, 2004, **357**, 4045-4056.
18. B. de Bruin, E. Bill, E. Bothe, T. Weyhermüller and K. Wieghardt, *Inorg Chem*, 2000, **39**, 2936-2947.
19. A. M. Tondreau, S. C. E. Stieber, C. Milsmann, E. Lobkovsky, T. Weyhermüller, S. P. Semproni and P. J. Chirik, *Inorg Chem*, 2013, **52**, 635-646.
20. D. P. Cladis, J. J. Kiernicki, P. E. Fanwick and S. C. Bart, *Chem Commun*, 2013, **49**, 4169-4171.
21. S. S. Galley, S. A. Pattenaude, C. A. Gaggioli, Y. S. Qiao, J. M. Sperling, M. Zeller, S. Pakhira, J. L. Mendoza-Cortes, E. J. Schelter, T. E. Albrecht-Schmitt, L. Gagliardi and S. C. Bart, *J Am Chem Soc*, 2019, **141**, 2356-2366.
22. W. J. Evans and M. A. Hozbor, *J Organomet Chem*, 1987, **326**, 299-306.
23. H. Sugiyama, I. Korobkov, S. Gambarotta, A. Moller and P. H. M. Budzelaar, *Inorg Chem*, 2004, **43**, 5771-5779.
24. N. H. Anderson, S. O. Odoh, U. J. Williams, A. J. Lewis, G. L. Wagner, J. L. Pacheco, S. A. Kozimor, L. Gagliardi, E. J. Schelter and S. C. Bart, *J Am Chem Soc*, 2015, **137**, 4690-4700.
25. D. Enright, S. Gambarotta, G. P. A. Yap and P. H. M. Budzelaar, *Angew Chem Int Edit*, 2002, **41**, 3873-3876.
26. A. M. Tondreau, S. C. E. Stieber, C. Milsmann, E. Lobkovsky, T. Weyhermüller, S. P. Semproni and P. J. Chirik, *Inorg Chem*, 2013, **52**, 635-646.



A Series of Reduced PDI neodymium complexes by the PDI ligand acting as an electron sink